Plasma Chem Plasma Process (2012) 32:781–799
DOI 10.1007/s11090-012-9376-x

ORIGINAL PAPER

Plasma Modification of Surface Wettability and Morphology for Optimization of the Interactions Involved in Blood Constituents Spreading on Some Novel Copolyimide Films

D. Popovici · A. I. Barzic · I. Stoica · M. Butnaru · G. E. Ioanid · S. Vlad · C. Hulubei · M. Bruma

Received: 17 November 2011 / Accepted: 9 April 2012 / Published online: 22 April 2012

Abstract Novel copolyimides (cPIs) based on 3,3′,4,4′-benzophenonetetracarboxylic dianhydride, 4,4′-diaminodiphenylmethane (DDM) and 1,6-diaminohexane (DAH) were synthesized. Their surface wettability was improved by plasma enhancement of polar component contribution to surface tension from 10 to 50 %. Interfacial energy reduction up to 2.07–2.95 mN/m was depicted in spreading work values that reveal the manner in which cPIs interact with blood constituents. The results showed that by increasing of the aliphatic DAH content in the polymer chain, the rejection of platelets is higher, prohibiting thrombosis and favoring cohesion with plasma proteins. The different water sorptions of the samples were evaluated by considering their morphologies and chemical affinities to water. When DAH prevails to DDM, water sorption capacity is lowered from 6.36 to 4.96 % db, presumably due to a higher chain packing efficiency. Atomic force microscopy data revealed that surface roughness is <8 nm for all polymers, even after plasma treatment, preventing clot formation.

Keywords Polyimide · Plasma · Surface properties · Water sorption · Biocompatibility

Introduction

Polyimides (PIs) are characterized by several outstanding properties, such as excellent mechanical strength and superior chemical and thermal resistance [1]. As a result, they have been extensively used in many applications, ranging from aerospace to microelectronics, optoelectronics, composites and membranes [1–3]. More recently, PIs were proven to be biocompatible [4, 5], and due to their appropriate mechanical properties, their

D. Popovici · A. I. Barzic (✉) · I. Stoica · G. E. Ioanid · S. Vlad · C. Hulubei · M. Bruma
"Petru Poni" Institute of Macromolecular Chemistry, 41A Grigore Ghica Voda Alley, 700487 Iasi, Romania
e-mail: irina_cosutchi@yahoo.com

M. Butnaru
Faculty of Medical Bioengineering, "Gr. T. Popa" University of Medicine and Pharmacy, 700115 Iasi, Romania

applications could be further extended to biomedical fields, as substrate/encapsulation materials in numerous bio-micro-electromechanical-systems (bio-MEMS) [6–8], or as microstructured substrates for contact guidance of osteoblast cell growth [9, 10]. However, in spite of having excellent combination of properties, most of conventional aromatic PIs have some drawbacks, e.g. insolubility in common organic solvents, intractability, infusibility and strong color that often limit their utility. For instance, in biomedical field, low dielectric constant, low refractive index, and high optical transparency along with good mechanical and thermal stability are the important properties required in bio-MEMS, blood-contact devices and cell culture substrates. In order to meet these demands, structural modification of these polymers often is essential. On the basis of the knowledge acquired from the structure–property relationships, a variety of cPIs have been molecularly designed [3, 11], but for an enhanced performance it is desired to choose biologically inert and nontoxic compounds, which exhibit stable mechanical, morphological and adhesion characteristics during exploitation. The combination of these factors assures the biocompatibility of the cPIs and implicitly the possibility of their existence in a living organism or in contact with living systems without negative consequences [12]. Comparatively to other aromatic tetracarboxylic dianhydrides used as raw materials for PIs, 3,3′,4,4′-benzophenone tetracarboxylic dianhydride (BTDA) is a unique bulky, photosensitive, and semi-flexible chemical structure, rendering new properties to the resulting compound [8, 13]. In addition, it was shown that BTDA is a biocompatible product used in preparation of composites highly adhesive to dentine [14] and in treatment of arthritis [15], making it applicable to a wider range of biomedical uses.

On the other hand, besides the bulk characteristics, cPIs bio-applications are affected by their low surface energy due to the absence of functional groups, which results in poor wettability [16]. Plasma technology, corona discharge and other techniques have been used to improve the wettability, printability, biocompatibility and other related surface properties [17–19], which are responsible for the resulting biological reactions. Since in most cases the biomaterial is in contact with aqueous environments in physiological situations, a better understanding of cells/tissues/proteins-biomaterial interactions can be achieved through interfacial water-polymer tension, which provides information on the intermolecular forces and the interfacial structure between two phases. When a polymeric material contacts blood or plasma, rapid protein adsorption and/or platelet adhesion takes place depending on the surface characteristics of the material. These unfavorable responses may cause discomfort to users, and sometimes require unwanted replacement of medical devices. In addition, these responses can initiate the activation of blood clotting cascade, which may be potentially fatal in many procedures using medical devices with large blood-contacting area [20, 21]. Therefore, interpretation of cPIs surface characteristics and precise control by physical and/or chemical modification should be significantly considered in designing them as biomaterials. Generally, their biocompatibility is mainly affected by surface characteristics including surface smoothness, distribution and functionality, and hydrophilic/hydrophobic balance of surface [22]. Therefore, contact angle measurement is one simple method to characterize the surface properties.

In a previous publication [23], some partially aliphatic copolyimides derived from 3,3′,4,4′-benzophenonetetracarboxylic dianhydride (BTDA), 4,4′-diaminodiphenylmethane (DDM) and 1,6-diaminohexane (DAH) were prepared and characterized from the view point of their chemical structure, thermal and mechanical behavior. The aim of this work is to improve the surface properties of some novel BTDA-derived cPIs, with different aliphatic content, by high frequency and low pressure air plasma. The biocompatibility of these compounds is investigated in the aspect of their blood compatibility, meaning the

interfacial tension and balance between adhesion and cohesion of blood cells and sanguine plasma proteins to the cPIs surface. In this context, the results were discussed in correlation with the morphology and chemical structure of the synthesized cPIs, comparing them to their respective homopolyimides (hPIs), in order to identify the optimal molecular aspects, which make them suitable for blood-contacting devices.

Experimental

Materials

Benzophenone-3,3‘,4,4′-tetracarboxylic dianhydride (BTDA, Aldrich) was recrystallized from acetic anhydride and vacuum dried before use. 4,4′ diaminodiphenylmethane (DDM, Sigma) was recrystallized from ethanol solution. 1,6 diaminohexane (DAH, Fluka) was used without further purification. *N*-methyl-2-pyrrolidone (NMP, Aldrich) was purified by distillation under reduced pressure and stored over 4Å molecular sieves. Scheme 1 shows the chemical structure of those monomers.

Polymer Synthesis

Polyimides (PIs) were synthesized by reacting BTDA with DDM and/or DAH. An equimolar ratio of diamine and dianhydride has been applied for preparation of the polymers. PIs (PI1 and PI5) and copolyimides (cPIs) (PI2–PI4) were synthesized via a two-step process by thermal imidization method in solution. The poly (amic acid)s (PAAs) were prepared in N-methylpyrrolidinone (NMP) ($\sim$15 %wt) and were not isolated.

A general polymerization procedure could be illustrated by the following example: 0.2974 g (1.5 mmol) of DDM and 0.1744 g (1.5 mmol) of DAH were dissolved in 8 mL anhydrous NMP in a 150 mL three-necked round bottom flask, fitted with a nitrogen inlet tube, a mechanical stirrer and a reflux condenser. 0.9667 g (3 mmol) of BTDA was rapidly added with stirring. Considerable gelation occurred during the addition of the dianhydride, which gradually disappeared on stirring at 35 °C for 2 h. The reaction mixture was stirred for a further 20 h at room temperature to yield viscous PAA solution. The PAA was subsequently converted into PI and cPI, by a thermal imidization process at 180–190 °C

Scheme 1 Polyimide monomer structures

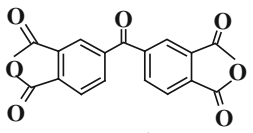

BTDA

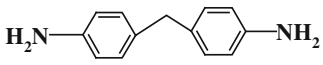

DDM

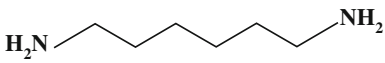

DAH

for at least 5 h. A slow nitrogen flow through the flask was continuously employed throughout the reaction. The reaction mixture was precipitated into methanol. The resulting powder was finally dried in an oven at 80 °C under reduced pressure for 4 h. All other polymers were synthesized by analogous procedure as described.

PI and cPI films were prepared through imidization of PAA films cast on a glass substrate, which were placed overnight in an 80 °C oven to remove most of the solvent. The semidried PAA films were further dried in an oven and transformed into PIs and cPIs, by the following heating program: 120, 160, 180, 210 and 270 °C for 1 h at each temperature. After stripping the films in hot water, the resulting samples were dried at 65 °C in a vacuum oven for 24 h. Completed imidization of all polymers was confirmed by IR spectroscopy. Solvent content was determined by thermogravimetric analysis to be <1 % (w/w).

Measurements

Infrared spectra were recorded with a Bruker Vertex 70 spectrometer in transmission mode, at 24 cm^{-1} resolution, by using precipitated polymers ground in potassium bromide pellets. Polymer solubility was determined at room temperature at a concentration of 1 % (w/v).

Thermogravimetric analyses (TGA) were performed on a MOM derivatograph (Hungary) in air, at a heating rate of 10 °C/min. The initial decomposition temperature (IDT) is characterized as the temperature at which the sample achieves a 5 % weight loss. The temperature of 10 % weight loss (T_{10}), was also recorded.

The static contact angles were measured by the sessile-drop method, with a CAM-101 (KSV Instruments, Helsinki, Finland) contact angle measurement system equipped with a liquid dispenser, video camera, and drop-shape analysis software, at room temperature. Double distilled water, ethylene glycol and methylene iodide were used as test liquids for these studies. For each kind of liquid, three different regions of the surface were selected to obtain a statistical result, taking into consideration the contact angle values of three measurements with an error of $\pm 1°$. The relative error on the calculated parameters was is in the range of 0.02–0.06 %.

The same types of samples were plasma-treated, by exposing the polymer films to a low temperature and low pressure glow discharge. Cold air plasma treatment was performed using an installation, done in our laboratories [24]. The installation used for producing plasma consists of a reactor, a liquid nitrogen trap, a vacuum pump, the whole set being connected to a command and control block. The pressure in the reaction vessel is adjusted by means of a needle valve and is measured with the pressure gauge. The reactor used for treatment of the materials is made of a Pyrex-glass vessel endowed with plane parallel aluminum electrodes. The piece that supports the samples subjected to treatment is set on a stainless steel grid placed between the electrodes. The high frequency (HF) discharge in the reaction vessel is ignited and maintained by the generator with the frequency of 1.2–13.5 MHz. In order to keep constant the HF glow discharge parameters during the treatments, the generator is equipped with a master oscillator with adjustable frequency within the range 1.2–1.5 MHz and a load tuned power amplifier. A control-command block adequately connected to magnet valves, pressure and temperature sensors, permits to establish the gas pressure and flow within the reactor. For the treatment of studied polyimides the following characteristics were used: electric field between the electrodes: 30 V/cm; frequency: 1.2 MHz; pressure: 0.24 mbar. Duration of the plasma exposure was of 10 min, the contact angles measurements being performed immediately after it.

Dynamic vapour sorption (DVS) measurements were performed on an IGAsorp apparatus (supplied by Hiden Analytical), with the following characteristics: minimum gas pressure of 2 bar; resolution of 0.1 μg for 100 mg and sample containers made out of stainless steel micron-sized mesh. Before sorption measurements, the samples were dried at 25 °C in a dry nitrogen flow (250 mL/min) until the weight of the sample was in equilibrium at a relative humidity (RH) <1 %. The vapour pressure was increased and decreased after an established program, which implies the variation with half a degree in the range of 0.5–90. Also, for sorption and desorption measurements, a program with 10 % humidity steps between 0 and 90 % RH was used, each having a pre-established equilibrium time between 40 and 50 min. The cycle was ended by decreasing the vapour pressure in steps to obtain also the desorption isotherms.

Blood cell attachment was determined using 0.1 ml of blood (human blood from healthy voluntary donors, collected on 3.8 % sodium citrate solution as anticoagulant in 9:1 v/v ratio) that was incubated with 1 cm^2 material surface area for 15 min at 37 °C and humidity. After the incubation period the films were washed three times with Phosphate Buffer Saline (PBS), and subsequently immersed for 10 min in formaldehyde 10 %. The removal of the fixing compound was made by rinsing the samples successively in distilled water and then in PBS. The surface of the samples was examined on an optical microscope (Olympus) in a PBS drop.

Atomic force microscopy (AFM) measurements were made on a scanning probe microscope solver pro-M platform (NT-MDT, Russia), in air, at room temperature, in tapping mode. A rectangular silicon cantilever NSG10 (NT-MDT, Russia), with a typical force constant $K_N = 11.8$ N/m and 156 kHz oscillation frequency was used. The tip curvature radius and height was 10 nm and 14–16 μm, respectively. The scan area was 1×1 μm^2 and for image acquisition and image analysis, the latest version of the NT-MDT NOVA software was used.

Results and Discussion

Polymer Synthesis

Polyimides were synthesized starting from a pair of diamines, DDM/DAH, and BTDA as dianhydride, by the ring-opening polyaddition at room temperature to PAAs, and imidization by sequentially heating process to the final polymers, PI1-PI5. Transformation from PAA to cPI was possible via the thermal cyclodehydration method. The chemical structures of the resulting polymers are presented in Scheme 2.

Figure 1 exemplifies the IR spectra of samples PI1, PI3 and PI5. The polymers show the characteristic imide absorption bands at around 1,775 cm^{-1} (attributed to the C=O asymmetrical stretching vibrations of imide groups) 1,712 cm^{-1} (attributed to the C=O symmetrical stretching vibrations of imide groups) 1,370 and 720 cm^{-1} (assigned to C–N stretching and C–N bending, respectively, in imide groups). An additional band, at 1,670 cm^{-1}, is attributed to C=O stretch of benzophenone. The absorptions at around 2,935 and 2,860 cm^{-1} are assigned to the CH_2 vibration of aliphatic units, while, the C–H linkage of aromatic rings shows a peak at about 3,050 cm^{-1}. The broad absorption band at 3,350–3,450 cm^{-1} characteristic of NH amidic and the narrow absorption peak at 1,650–1,660 cm^{-1} due to C=O group in amide linkage disappeared entirely, indicating the completion of thermal imidization of the intermediate PAA into final polyimide structure and confirms the synthesis of polymers.

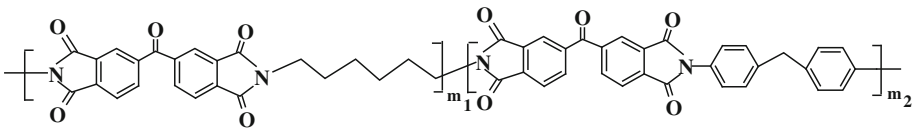

PI1 - PI5

PI (composition: % diamine)	PI1	PI2	PI3	PI4	PI5
DAH	0	25	50	75	100
DDM	100	75	50	25	0

Scheme 2 Chemical structures of investigated polymers

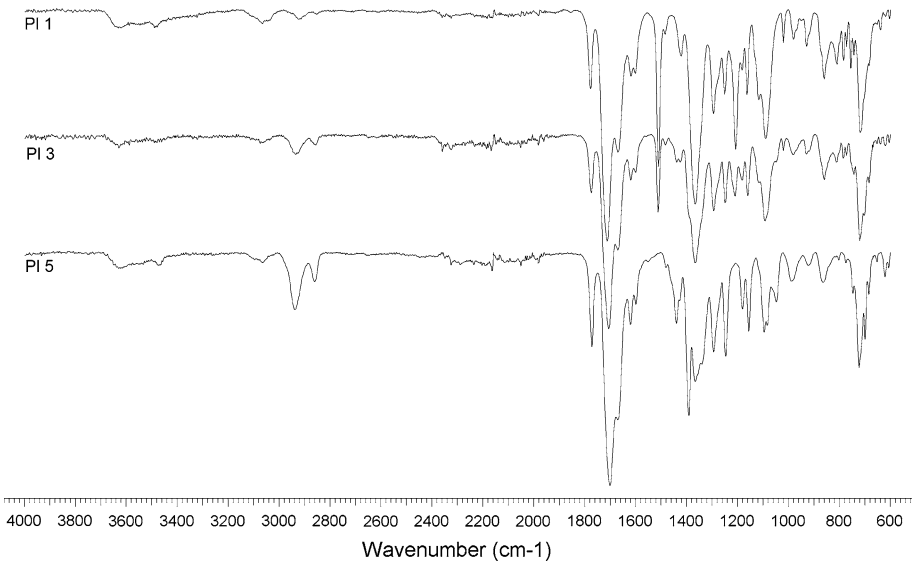

Fig. 1 FTIR spectra of PI1, PI3 and PI5 films

Surface Wettability and Interfacial Energy

The surface free energy of a polymer can be derived from contact angle measurements in the advancing, receding, and preferred wetting modes using equations of the molecular theory of wetting. An approach of the sample surface energy is a consideration of sample surface tension, which according to the components approach, it given by a combination of dispersion forces (van der Waals forces) and polar forces (hydrogen bonding). The acid–base theory was developed by van Oss, Chaudhury and Good [25–27] as they tried to relate the surface tension components more closely with their chemical nature. The polar component describes the acid–base interactions instead of hydrogen bonds, while the non-polar term describes London–van der Waals forces instead of dispersion interactions. Thus, the surface tension could be described by Eqs. (1–3):

$$1+\cos\theta=\frac{2}{\gamma_{lv}}\cdot\left(\sqrt{\gamma_{sv}^{LW}\cdot\gamma_{lv}^{LW}}+\sqrt{\gamma_{sv}^{+}\cdot\gamma_{lv}^{-}}+\sqrt{\gamma_{sv}^{-}\cdot\gamma_{lv}^{+}}\right) \quad (1)$$

$$\gamma_{sv}^{AB}=2\cdot\sqrt{\gamma_{sv}^{+}\cdot\gamma_{sv}^{-}} \quad (2)$$

$$\gamma_{sv}^{LW/AB}=\gamma_{sv}^{LW}+\gamma_{sv}^{AB} \quad (3)$$

where superscripts "*LW*" and "*AB*" indicate the disperse and the polar component obtained from the γ_{sv}^{-} electron-donor and the γ_{sv}^{+} electron-acceptor interactions.

As to Eq. (1), literature data [27–29] indicate that three polar liquids and a set of three equations may be used, if the values of the liquids parameters are not too close. Della Volpe et al. [30] show that an improper utilization of the three liquids, without dispersive liquids, or with two prevalently basic or prevalently acidic liquids strongly increases the ill-conditioning of the system. The different estimates of the acid–base components, obtainable for the same solid by different triplets of liquids, do not necessarily imply that this method is inconsistent, but may simply reflect the large inaccuracies affecting the results, as due to ill-conditioning. Also, literature postulated [27] that contact angles should be measured with a liquid of surface tension higher than the anticipated solid surface tension. Eq. (1), written for three liquids, leads to a three equation system for determining the surface tension components. In our investigation, the solid surface tension components γ_{sv}^{LW} and γ_{sv}^{AB} were determined from a simplified equation system, in which are introduced the parameters of two polar liquids and a non-polar one (Table 1), and the contact angles from Table 2. The surface tension components of the test liquids, namely water, ethylene glycol and methylene iodide were taken from literature [31–33], and presented in Table 1.

Table 3 lists the obtained values of surface tension components and electron-donor and electron-acceptor parameters, before and after plasma treatment. For untreated samples, the non-polar component, γ_{sv}^{LW}, increases as the aliphatic DAH moieties in the polymer chain, prevail comparatively with aromatic DDM moieties, while the polar component, γ_{sv}^{AB} decreases. This could be due to the reduction of charge transfer interactions from the aromatic sequences (BTDA, DDM) by the presence of DAH units, and thus lowering the polarity of the polyimide from PI1 to PI5.

Table 1 Dispersion and polar contributions to the surface tension mN/m) of various test liquids and some biological materials

	γ_{lv}	γ_{lv}^{d}	γ_{lv}^{p}	γ_{lv}^{+}	γ_{lv}^{-}
Test liquids					
Water [31]	72.80	21.80	51.00	25.50	25.50
Methylene iodide [32]	50.80	50.80	0.00	0.72	0.00
Ethylene glycol [33]	48.00	29.00	19.00	1.92	47.00
Biological materials					
Blood [49, 50]	47.50	11.20	36.30	–	–
Fibrinogen [51]	41.50	37.60	3.89	0.10	38.00
IgG [52]	51.30	34.00	17.30	1.50	49.60
Albumin [49, 50]	62.50	26.80	35.70	6.30	50.60
Red blood cells [53]	36.56	35.20	1.36	0.01	46.20
Platelet [53]	118.24	99.14	19.10	12.26	7.44

Table 2 Contact angles of different liquids on polyimide films (°), before and after plasma treatment

Sample	Untreated samples			Plasma treated samples		
	Water	Ethylene glycol	Methylene iodide	Water	Ethylene glycol	Methylene iodide
PI1	80	55	52	33	12	59
PI2	82	57	48	35	13	58
PI3	84	60	45	36	15	57
PI4	87	62	44	37	16	56
PI5	89	63	42	39	17	56

Table 3 Surface tension components and electron-donor and electron-acceptor parameters (mN/m) for untreated and plasma treated samples

Sample	Untreated samples					Plasma treated samples				
	γ_{sv}^{LW}	γ_{sv}^{-}	γ_{sv}^{+}	γ_{sv}^{AB}	$\gamma_{sv}^{LW/AB}$	γ_{sv}^{LW}	γ_{sv}^{-}	γ_{sv}^{+}	γ_{sv}^{AB}	$\gamma_{sv}^{LW/AB}$
PI1	29.49	7.60	0.47	3.80	33.29	20.61	51.07	3.64	27.28	47.89
PI2	31.88	6.40	0.21	2.34	34.22	21.37	48.59	3.50	26.10	47.47
PI3	33.63	5.73	0.05	1.02	34.65	21.94	47.67	3.27	24.98	46.92
PI4	34.62	4.14	0.02	0.45	35.07	22.02	46.70	3.24	24.59	46.61
PI5	36.02	3.11	0.01	0.07	36.09	22.71	44.14	3.10	22.99	45.70

Biocompatibility of the investigated polymers can be improved through changes in polarity and wettability, incorporation of surface functional groups that help prevent thrombogenicity, and surface coatings of biologically compatible species, such as proteins and antibiotics. Plasma treatment is a technique that can be used to modify the surface properties of biomaterials without also altering bulk properties that affect their function [34, 35]. High frequency (HF) plasma offers a unique route for surface patterning results in a smooth, pinhole-free ultrathin films. From this reason, in order to optimize the surface properties and implicitly the biocompatibility of studied samples [36], they were subjected to HF cold-plasma treatment. This type of processing implies low energy processes and the created species have little penetrating energy. Thus, the modification is limited to the surface typically no deeper than a few molecular layers, providing specific functionality and long-term stability. The various excitation, ionization and dissociation reactions in the plasma generate high-energy and reactive species (electrons, ions, radicals, photons) that interact with polymer film surface, changing its chemical and physical characteristics. The type of surface modification induced by plasma treatment is strongly dependent on the choice of reactive gas. Reactive gas plasmas involving gases such as oxygen, nitrogen and carbon dioxide or their mixtures (air—the present case), introduce new functional groups onto the PI surface [37]. In particularly, the presence nitrogen from air plasma leads to the formation of C–N–C, C–N and N=C=N groups, the latter one being able to activate carboxyl groups [38]. Also, nitrogen from the plasma conducts to decrease of the bonding percentage, related to normal nitrogen bonding (O=C–N–C=O) in the polyimide structure, and to its conversion into C–N–C bonding [39]. The traces of CO_2 from air plasma treatment of PI induce the cleavage of imide groups to form COOH and amide groups [40].

Air plasma treatment is very effective to crack the C–O–C or C=O bonds in PIs, and to produce many dangling oxygen bonds [37, 41, 42]. The oxygen from air plasma bombardment of PI film can cause some atoms to be sputtered away and substituted by oxygen atoms. This substitution produces highly polar groups (hydroxyls, carbonyls, and in some cases carboxylic groups) at the surface by breaking the imide and benzene rings and forming new polar species of C–O and C–N–C, and raises the surface polarity and wettability [43]. The biological efficacy of the air plasma is usually attributed to reactive species, such as hydroxyl groups and atomic oxygen, and the use of atmospheric air rather than noble gas greatly enhances their generation. One of the most efficient results of such type plasma treatment is increased wettability of the surface, which is thought to be limited by the competition of chain scission (etching) and functional modification of the surface. Thus, plasma treatment increases the number of Lewis acid–base sites. In an acid–base perspective, oxygen containing functionalities increase the strength of the Lewis acid–base interaction with water and other polar liquids. These groups give both an electron-donor character through the electron lone pair of oxygen and an electron-acceptor character through the active hydrogen linked to the electronegative oxygen atoms [44].

In case of studied cPIs, the values of γ_{sv}^{LW} decrease by the plasma treatment, while those of γ_{sv}^{AB} increase, leading to higher total surface tensions compared to those of the untreated samples. This observation also arises from Table 2, which presents the results for relatively hydrophobic surfaces (with high contact angles) that were converted into more hydrophilic surfaces (with low contact angles), by plasma treatment of studied samples. Plasma treatment results in a dramatic decline of the contact angle and a corresponding increase of the polymer wettability. The increase of the latter parameter is caused by the creation of polar groups at the polymer surface, which exhibit high hydrophilicity. Aging of the plasma treated polymers is accompanied by an increase of the contact angle which is due to a reorientation of the molecular segments, produced by the plasma treatment, due to their interaction with ambient atmosphere [45]. Major role in this process has the orientation of the polar groups toward the polymer bulk. It is well known that the contact angle is mostly affected by the chemical structure and morphology of the polymer surface layer, especially by the presence of oxidized degradation products [45]. A recent study shows that a good wettability stable in time of PI films can be achieved by coating polymer surface with silicon oxide [46]. In this context, our future studies will be focused on stabilization of surface characteristics of synthesized cPIs induced by plasma exposure in order to extent their utility to biomedical fields.

In contact with physiological aqueous environments, intermolecular forces occurring at the interface with these compounds can be described by the interfacial tension, γ_{sl}, calculated with Eq. (4):

$$\gamma_{sl} = \left(\sqrt{\gamma_{lv}^{p}} - \sqrt{\gamma_{sv}^{p}}\right)^2 + \left(\sqrt{\gamma_{lv}^{d}} - \sqrt{\gamma_{sv}^{d}}\right)^2 \tag{4}$$

The values of interfacial tension of studied cPI films at the water interface, γ_{sw}, are presented in Table 4. It can be observed that the interactions at the interface are more pronounced as the aliphatic moieties content increases in the polymer chain (from PI1 to PI5), while after plasma exposure the values of γ_{sw} decrease. Also, these effects include the surface free energy, ΔG_w, expressing the balance between hydrophilicity and hydrophobicity on the surface. The ΔG_w values were obtained from Eq. (5) [47] by using the total surface tension of water, γ_{lv}, from Table 1, and the contact angle of water for the studied samples, θ_{water}, from Table 2.

Table 4 Interfacial tension solid-water, free energy of hydration, and interfacial tension solid-blood values before and after plasma treatment

Sample	γ_{sw} (mN/m)		ΔG_w(mJ/m^2)		γ_{sb} (mN/m)	
	Untreated	Plasma treated	Untreated	Plasma treated	Untreated	Plasma treated
PI1	27.54	3.70	−85.44	−133.86	20.95	2.07
PI2	32.45	4.13	−82.93	−132.43	25.50	2.46
PI3	38.87	4.60	−80.41	−131.69	31.17	2.84
PI4	43.35	4.76	−76.61	−130.94	35.10	2.95
PI5	49.07	5.52	−74.07	−129.38	40.23	3.38

$$\Delta G_w = -\gamma_{lv} \cdot (1 + \cos\theta_{\text{water}}) \tag{5}$$

Generally, the literature [29, 47] mentions that, for $\Delta G_w < -113$ mJ/m, the polymer can be considered more hydrophilic while, when $\Delta G_w > -113$ mJ/m, it should be considered more hydrophobic. Thus, the results from Table 4, the interfacial tensions between polymer-water, γ_{sl}, and the surface free energy, ΔG_w, reveal that the studied polymers possess an increased wettability after plasma treatment cleans the surface and implicitly a high hydrophilicity, property useful for biomedical applications.

Studies pertaining to development of blood compatibility criteria demonstrated that the behavior of a material in a biological medium is dictated by the interfacial energy at the polymer-blood interface [48]. The concept for blood-compatible materials starts from considerations of minimizing the thermodynamic driving force for the adsorption of blood components, as well as maintaining a mechanically stable blood-biomaterial interface. In order to reconcile these two requirements, a blood-biomaterial interfacial tension of 1–3 mN/m is considered satisfactory [48]. Using a simplified model, it is shown that the above criterion can be satisfied when the polar and dispersion surface free energy components of a biomaterial are separately sufficiently near to their respective surface-free energy counterparts of blood. As a result of this condition, even solids which differ appreciably in their total surface free energies can remain equally compatible with blood. For these BTDA-derived cPIs the interfacial tension with blood, γ_{sb}, was obtained with Eq. (4), in which we substituted the values for blood surface tension components taken from the literature [49, 50] as listed in Table 1. The results indicate that untreated samples exhibit higher values than those predicted by the biocompatibility criteria. Also, γ_{sb} values are increasing as the aliphatic DAH moieties content in the polymer chain prevail compared to aromatic DDM moieties, and they are strongly decreasing after plasma treatment. It can be observed that all samples, excepting polyimide PI5, present values framed in 2.07–2.95 range, which are in agreement with blood compatibility criteria. Thus, combining this aspect with a high transparency and flexibility induced by the aliphatic sequences from DAH, it can be assessed that copolyimide PI4 is the most suitable in applications for blood-contacting materials (like surfaces of vessel grafts, membrane oxygenators, and extracorporeal circuits).

Blood-Copolyimide Interactions

Hemocompatibility is a major issue in biomedical systems design. Materials used for these devices must not interact unfavorably with blood. One major aspect of hemocompatibility

is the ability of a surface to resist the deposition of proteins from the blood onto the surface. Protein deposition triggers clotting and can cause the device to function improperly or fail outright. This is unacceptable in biomedical applications where device robustness is paramount. For a deeper understanding of the interactions that occur in blood-biomaterial surface, the influence of different blood components to the polymer surface has to be evaluated. The balance between adhesion, W_a, and cohesion, W_c, of blood constituents on studied samples can be described by work of spreading, $_{Ws}$, expressed in Eq. (6):

$$W_s = W_a - W_c = 2 \cdot \left[(\gamma_{sv}^{LW} \cdot \gamma_{lv}^{d})^{1/2} + (\gamma_{sv}^{+} \cdot \gamma_{lv}^{-})^{1/2} + (\gamma_{sv}^{-} \cdot \gamma_{lv}^{+})^{1/2} \right] - 2 \cdot \gamma_{lv} \qquad (6)$$

In order to analyze the possibility of using these BTDA-derived cPIs in biomedical applications and for establishing their compatibility with blood, in Eq. (6) were introduced the surface tension parameters of fibrinogen [51], albumin [49, 50], immunoglobulin IgG [52], red blood cells [53] and platelets [53]. When blood is brought in contact with a foreign polymer surface, adsorption of specific proteins from sanguine plasma and/or cell adhesion occurs. Depending on the surface characteristics of the material, the extent of adhesion decides its life, as cellular adhesion to biomaterial surface could activate coagulation and the immunological cascades. Therefore, cellular adhesion has a direct bearing on the thrombogenicity and immunogenicity of a biomaterial and thus dictates its blood compatibility. In this paper, we suggest the work of adhesion of the blood cells, namely erythrocytes (RBC) and platelets, as parameters for characterizing biomaterials versus cell adhesion. Thus, the materials which exhibit a lower work of adhesion would lead to a lower extent of adherent cells than those with a higher work of adhesion. Table 5 shows positive values for red blood cells work of spreading, W_{RBC}, suggesting a higher work of adhesion compared to the work of cohesion. Before plasma treatment PI1 and PI2, with more aromatic content, exhibit an adhesion with red blood cells, while for ratios larger than 50 % of DAH content in the polymer structure, a small cohesion is obtained. After plasma exposure the values of spreading coefficient are positive, revealing a small increase of adhesion, which for copolyimides PI2–PI4 is slightly reduced as the DAH content is increased. Regarding the exposure to platelets, the negative values of spreading work, W_{plat}, indicate that all samples present a pronounced cohesion, maintained after plasma

Table 5 Work of spreading (mN/m) values of different blood components on untreated and plasma treated samples

Samples	W_{fib}	W_{IgG}	W_{alb}	W_{RBC}	W_{plat}
Untreated samples					
PI1	−6.21	−22 .86	−45.18	1.19	−105.29
PI2	−6.51	−24.10	−47.32	0.61	−103.83
PI3	−7.61	−25.96	−49.76	−0.79	−103.01
PI4	−7.81	−27.00	−51.85	−0.97	−104.29
PI5	−7.05	−26.88	−52.59	−0.19	−104.07
Plasma treated samples					
PI1	0.72	−5.28	−14.98	8.11	−85.62
PI2	1.17	−5.26	−15.53	8.56	−85.40
PI3	1.11	−5.59	−16.12	8.42	−84.98
PI4	1.06	−5.78	−16.50	8.39	−85.36
PI5	1.35	−5.95	−17.26	8.69	−85.45

treatment. This result suggests that studied BTDA-derived polymers do not interact with platelets and thus prevent activation of the coagulation at the blood/biomaterial interface.

Another important problem in evaluation of biocompatibility consists in analysis of the competitive adsorption behavior of blood proteins at the biomaterial surface, since it determines the pathway and the extent of intrinsic coagulation and adhesion of platelets. Predictions about the interactions between the biomaterial surface and the adsorbed proteins can only be formulated by having an exact knowledge of the structure of the biomaterial's surface. For untreated samples the spreading work values for fibrinogen, albumin and IgG are negative revealing that cohesion prevails and thus favoring a non-adsorbent behavior at the interface, as required by bio-applications. Plasma treatment maintains this result, but even in case of fibrinogen for which the values of W_{fib} become positive, they are very small, consequently suggesting that this soluble plasma glycoprotein will hardly lead to blood coagulation. Among the plasma modified samples the polyimide PI1 and copolyimide PI4 exhibit the lowest values of W_{fib}, which along with the rejection of platelets, have a significant role in prohibiting thrombus formation. From this point of view, the investigated materials can be considered as blood compatible since their interaction with blood cells would not cause either any damage of blood cells or any change in the structure of plasma proteins. Therefore, it can be concluded that these materials fulfill the main requests of biocompatibility. In particularly, plasma exposed PI4 exhibit an optimal combination of flexibility and transparency (due to its high aliphatic content), of suitable cohesion with sanguine plasma proteins and platelets, of small adhesion with red blood cells; these results recommending it as a promising material for blood-contacting devices.

Clinical studies which have been performed on these samples revealed that at the polymer/blood interface there is no excessive platelets aggregation and RBC lysis. Also, as shown in optical microscopy images from Fig. 2 the presence of the studied compounds do not damage the morphology of the blood components, which is a positive indicative of a hemocompatible material [54]. More detailed investigations on these polyimides from the medical point of view will be the subject of a future work.

Water Uptake

In blood plasma composition, water is a prevailing element and therefore it is of great importance to evaluate the water uptake behavior of analyzed samples, since the swelling of the films could affect the performance of the blood-contacting devices in which they are implemented.

Water sorption behavior of cPIs was analyzed using moisture sorption isotherms. The role played by water molecules in the sample was interpreted on the basis of two models, Brunauer-Emmet-Teller (BET) [55] and Guggenheim–Anderson de Boer (GAB) [56–58], which allow a good fit of the water sorption data. The BET model is the most widely used technique for predicting moisture sorption by solids, especially to evaluate the surface area of solid materials. Generally, this method describes the isotherms until a relative humidity of 50 %, depending on the type of material and on the type of sorption isotherm [58]. This model is limited because it cannot describe very well the water sorption in multilayer. On the other hand, GAB approach is based on some modified assumptions of the BET model. It is presumed that there is an intermediate layer, which has different adsorption, and liquefaction heats and also that there is a finite number of adsorption layers. GAB model is used for finding out the monolayer sorption values and for determinations of solid surface

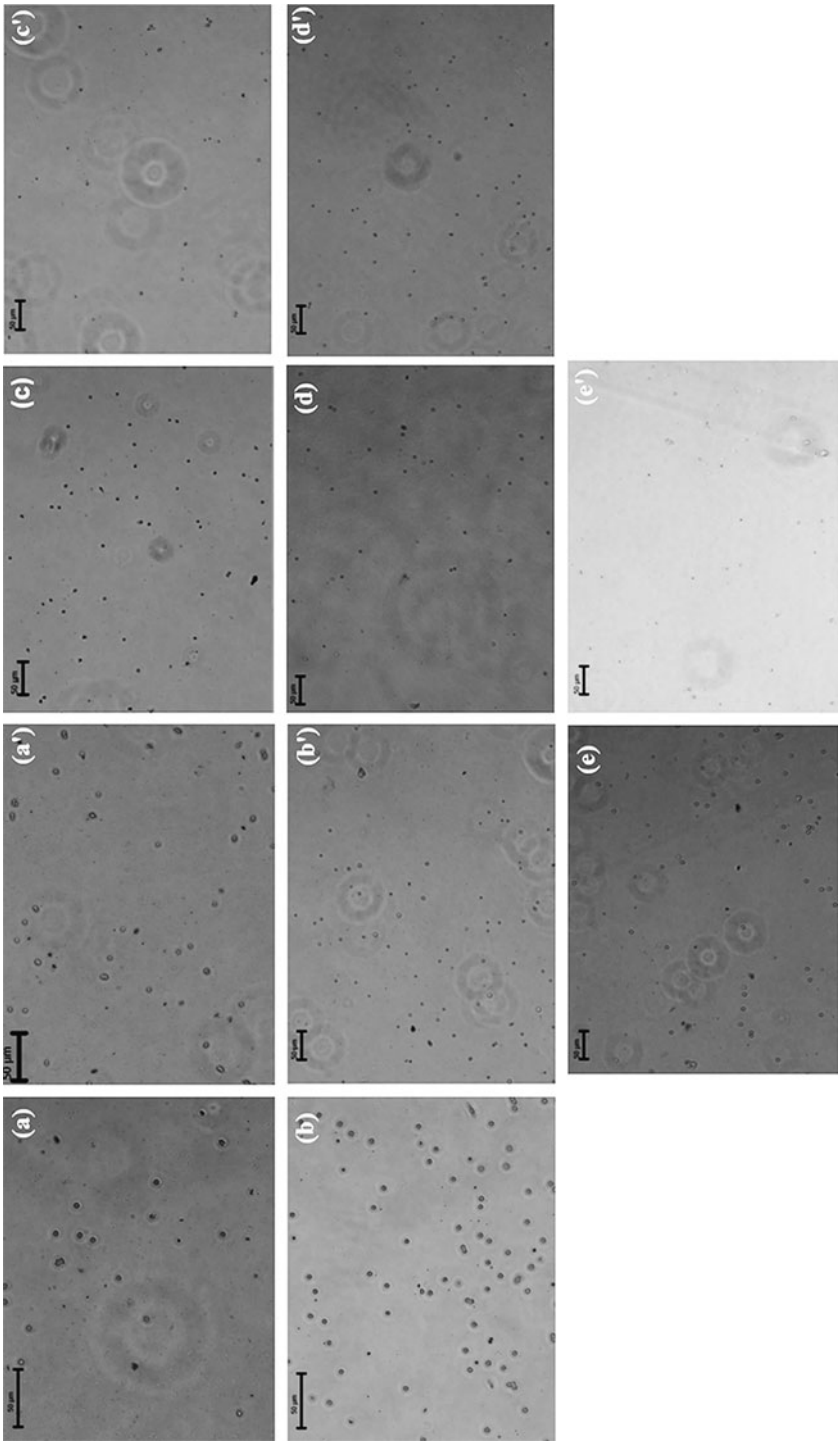

Fig. 2 Optical microscopy images of the blood components casted on the investigated polyimide surfaces (**a**)–(**e**) untreated and (**a'**)–(**e'**) plasma treated

area. The GAB equation covers a larger range of humidity conditions. The BET (7) and GAB (8) equations are very often used for modeling of the sorption isotherms

$$W = \frac{W_m \cdot C \cdot \frac{p}{p_0}}{\left(1 - \frac{p}{p_0}\right) \cdot \left(1 - \frac{p}{p_0} + C \cdot \frac{p}{p_0}\right)} \tag{7}$$

$$W = \frac{W_m \cdot C \cdot K \cdot \frac{p}{p_0}}{\left(1 - K \cdot \frac{p}{p_0}\right) \cdot \left(1 - K \cdot \frac{p}{p_0} + C \cdot K \cdot \frac{p}{p_0}\right)} \tag{8}$$

where: W—the weight of adsorbed water, W_m—the weight of water forming a monolayer, C—the sorption constant, p/p_0—the relative humidity, and K—the additional constant for the GAB Eq. (8).

Both of these methods have been used in many fields where the theory of mono and multilayer adsorption is very applied to the water sorption in order to find useful information about the compounds. Contrarily to the GAB model, which represents the sorption isotherm on a wide range of water activity values (a_w), the BET model enables the representation of the sorption isotherms only in a range of activities from: 0 to 0.35 according to Brunauer [55]. For water activities lower than 0.35, the BET model is better fitting the experimental results than the GAB model.

The shapes of the isotherms for the studied samples are isotherms of type III after IUPAC classification [59]. This type of adsorption is characteristic for porous solids [60]. In the case of adsorption, where capillary condensation occurs, hysteresis appears and is typical for systems with a very weak adsorbent-adsorbate interaction. The explanation of hysteresis is based on a change of geometry during the adsorption and desorption process. This is a sorption isotherm specific for a low hydrophilic material. The form of the moisture sorption isotherm is a sigmoidal shape curve with a point of inflection [61].

Knowing the density of adsorbed phase and using the relationship between pore volume and moisture uptake, an approximate value of the average pore size r_{pm}, can be established starting from Eq. (9). The relationship between the liquid volume, V_{liq}, and the percentage uptake, n, is:

$$V_{liq} = \frac{n}{100 \cdot \rho_a} \tag{9}$$

where ρ_a is the adsorbed phase density.

The average pore size can be calculated from the pore volume, assuming cylindrical pore geometry, according to Eq. (10):

$$r_{pm} = \frac{2 \cdot V_{liq}}{A} \tag{10}$$

where A is the BET surface area.

Combining equations (9) and (10), average pore size can be expressed with relationship (11):

$$r_{pm} = \frac{2 \cdot n}{100 \cdot \rho_a \cdot A} \tag{11}$$

According with the IUPAC classification [59], the PI samples have the average pore size appropriate for the nanoporous material range. The obtained data from sorption/desorption isotherms are summarized in Table 6.

Table 6 The main surface parameters of investigated samples, evaluated by sorption isotherms

Sample	Water vapours sorption capacity (% db)	BET analysis		GAB analysis		Average pore size (nm)	
		Monolayer (g/g)	Area (m^2/g)	Monolayer (g/g)	Area (m^2/g)	BET	GAB
PI 1	6.366	0.0157	55.136	0.0152	53.249	2.31	2.39
PI 2	5.244	0.0132	46.214	0.0146	51.147	2.26	2.05
PI 3	4.664	0.0116	40.812	0.0124	43.649	2.28	2.14
PI 4	4.595	0.0114	39.833	0.0122	42.757	2.30	2.15
PI 5	4.962	0.0139	48.617	0.0166	58.236	2.04	1.70

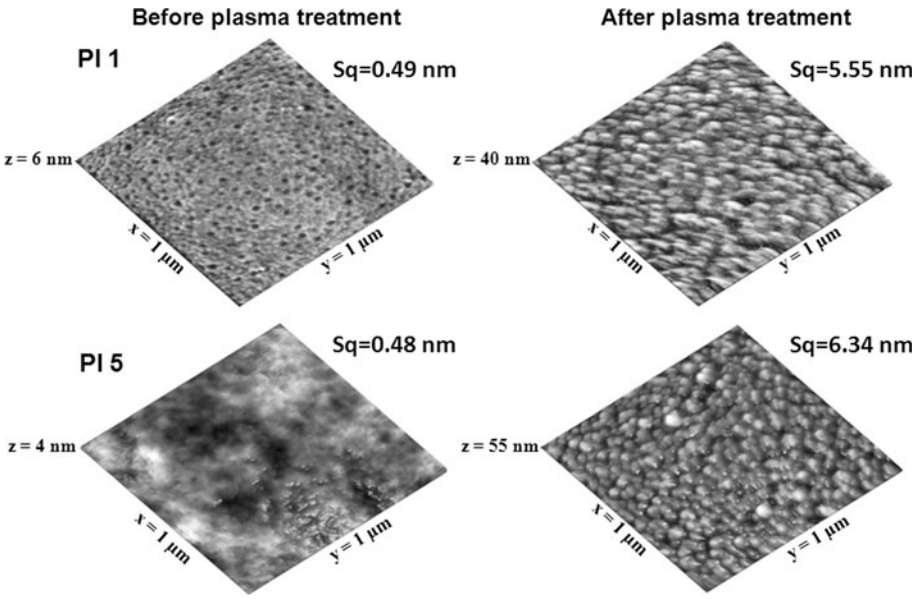

Fig. 3 AFM images of BTDA-derived polyimides PI1 and PI5 before and after plasma treatment

The differences between the water sorptions of the compounds are interpreted by considering the differences in their morphologies and chemical structure. The results indicate that by adding a larger amount of aliphatic DAH moieties in the polymer backbone, water vapours sorption capacity of the cPIs is diminished, presumably due to an increase in chain packing efficiency from PI2 to PI4. As observed in Table 6, PI4 film exhibits the lowest swelling degree, recommending its applicability in blood-contacting devices.

Surface Morphology

Besides the surface wettability and interfacial energy, the morphology of investigated samples determines the interactions occurring at the interface. Atomic force microscopy (AFM) was used to examine surface of the analyzed films and to measure their surface topography. Figures 3 and 4 present the three-dimensional images of the polyimides PI1

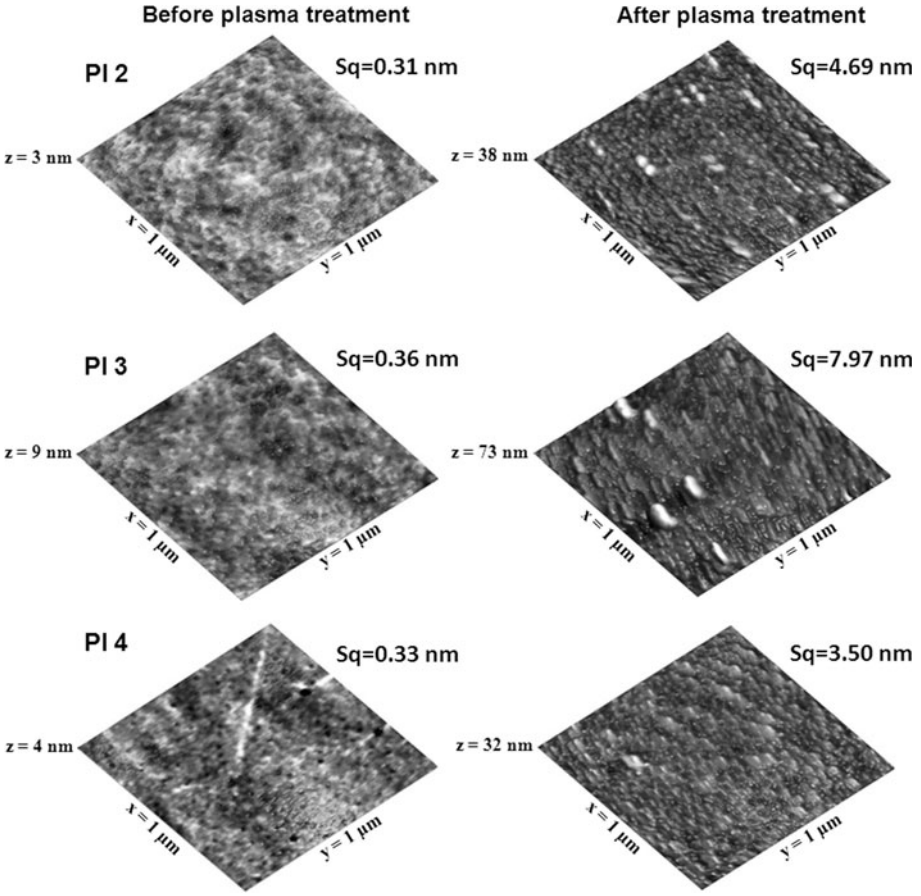

Fig. 4 AFM images of BTDA-derived copolyimides PI2-PI4 before and after plasma treatment

and PI5, and of the copolyimides PI2-PI4, respectively. The surface morphology and roughness of the polyimide film derive mainly from the characteristics of the polymer chains that govern aggregation and molecular ordering, which occur during drying and the thermal imidization processes. The untreated films reveal a uniform and flat surface morphology. When the films are examined at nanoscale, the surface shows a small root-mean-square roughness, *Sq*, framed between 0.31 and 0.49 nm. The low roughness values obtained for the studied polymers are comparable with other polyimides [62, 63].

The plasma treatment affects the polymer surface, generating new chemical groups and modification of the morphological structures. Thus, plasma intensifies roughness, a phenomenon which remains constant in time, so that nanometer-scaled granules appear on the films surface. This can be observed in AFM images, which reflect slightly higher values of *Sq*, comprised in the range of 3.50–7.97 nm. AFM data support the conclusion that enhancement in roughness is generated by a structural peculiarity of the PIs and cPIs obtained by introducing different diamine structures in the synthesis, and by plasma treatment, as well. Thus, the combination of flexible aliphatic DAH moieties with semi-rigid DDM ones, leads to decrease of roughness and, implicitly, determines better adhesion

of the BTDA-derived copolyimide films. A commonly accepted fact is that a low surface roughness leads to a good compatibility of the material. Reefs which disturb the laminar blood flow, as well as poststenotic turbulence, in particular, can cause clot formation [[64], [65]]. In the case of our samples, the plasma induces an increased roughness, but considering its order of magnitude it is still in the limits required by the biocompatibility. As observed in Fig. 4, the copolyimide PI4 exhibits the most adequate morphology for the pursued applications.

Conclusions

New BTDA-based copolyimides, with different content of flexible aliphatic DAH, were investigated to obtain information on their hydrophilic/hydrophobic properties, and to determine their interaction with blood cells and plasma specific proteins. High frequency and low plasma treatment influenced the surface tension parameters, interfacial free energy and work of spreading of blood constituents, increasing the surface hydrophilicity characteristics and decreasing interfacial tension with blood in the range of 2.07–2.95 mN/m, in accord with the biocompatibility criteria for PI1-PI4 samples. The results have reflected capacity of DAH moieties to lower the electron-donor character of polar contribution to surface tension, while maintaining a small adhesion of polymer films to red blood cells and a proper cohesion to platelets and albumin, fibrinogen and IgG. The differences between the water sorptions of the samples are influenced by their chemical structure, indicating a lower capacity as the flexible aliphatic DAH moieties amount in the polymer chain is higher.

The AFM images showed a uniform and flat surface morphology for untreated samples ($Sq = 0.31$–0.48 nm), changing into a granular structure after plasma treatment. The values of the root-mean-square roughness of all films are ranging between 3.50 and 7.97 nm, after plasma exposure, being favorable for laminar blood flow, preventing poststenotic turbulence and clot formation. In particular, plasma treated copolyimide PI4 presents a reduced roughness, an interfacial tension with blood of 2.95 mN/m, respecting the biocompatible criteria and the most suitable balance between adhesion/cohesion with blood components and the lowest capacity of swelling (4.59 % db), aspects which recommend it as potential material for blood-contacting devices.

Acknowledgment One of the authors (A. I. Barzic) is grateful for the financial support offered by the European Social Fund—"Cristofor I. Simionescu" Postdoctoral Fellowship Programme (ID POSDRU/89/1.5/S/55216), Sectorial Operational Programme Human Resources Development 2007–2013.

References

1. Ghosh MK, Mittal KL (1996) Polyimides: fundamentals and applications. Marcel Dekker Inc, New York
2. Kim SI, Ree M, Shin TJ, Jung JC (1999) J Polym Sci Part A 37:2909–2921
3. Mathews AS, Kim I, Ha C-S (2007) Macromol Res 15:114–128
4. Richardson RR Jr, Miller JA, Reichert WM (1993) Biomaterials 14:627–635
5. Stieglitz T, Beutel H, Schuettler M, Meyer JU (2000) Biomed Microdev 2:283–294
6. Cheung KC, Renaud P, Tanila H, Djupsund K (2007) Biosens Bioelectron 22:1783–1790
7. Mercanzini A, Cheung K, Buhl DL, Boers M, Maillard A, Colin P, Bensadoun JC, Bertsch A, Renaud P (2008) Sens Actuators A 143:90–96

8. Myllymaa S, Myllymaa K, Korhonen H, Töyräs J, Jääskeläinen JE, Djupsund K, Tanila H, Lappalainen R (2009) Biosens Bioelectron 24:3067–3072
9. Charest JL, Bryant LE, Garcia AJ, King WP (2004) Biomaterials 25:4767–4775
10. Nagaoka S, Ashiba K, Kawakami H (2002) Artif Org 26:670–675
11. Hasegawa M, Horie K (2001) Prog Polym Sci 26:259–335
12. Ruckenstein E, Gourisankar SV (1986) Biomaterials 7:403–422
13. Fang X-Z, Li Q-X, Wang Z, Yang Z-H, Gao L-X, Ding M-X (2004) J Polym Sci A 42:2130–2144
14. Bowen RL (1987) Simplified method for obtained strong adhesive bonding of composites to dentin, enamel and other substances, US Patent no. 4,659
15. Nguyen TT (1994) Acidic polysaccharides crosslinked with polycarboxylic acids and their uses, US Patent no. 08/362,689
16. Yang GH, Kang ET, Neoh KG, Zhang Y, Tan KL (2001) Coll Polym Sci 279:745–753
17. Cui N, Brown MD (2002) Appl Surf Sci 189:31–38
18. Suzer S, Argun A, Vatansever O, Oral O (1999) J Appl Polym Sci 74:1846–1850
19. Hiraoka H, Lasare S (1990) Appl Surf Sci 46:264–271
20. Clarke S, Davies MC, Roberts CJ, Tendler SJB, Williams PM, O'Byrne V, Lewis AL, Russell J (2000) Langmuir 16:5116–5122
21. van Delden CJ, Engbers GHM, Feijen J (1996) J Biomater Sci Polym Ed 7:727–740
22. Elam JH, Nygren H (1992) Biomaterials 13:3–8
23. Cristea M, Ionita D, Hulubei C, Timpu D, Popovici D, Simionescu BC (2011) Polymer 52:1820–1828
24. Ioanid GE (2005) Rom J Phys 50(9–10):1071–1079
25. van Oss CJ, Good RJ, Chaudhury MK (1988) Langmuir 4:884–891
26. van Oss CJ, Ju L, Chaudhury MK, Good RJ (1988) Chem Rev 88:927–941
27. van Oss CJ (1994) Interfacial forces in aqueous media. Marcel Dekker Inc, New York
28. Good RJ, van Oss CJ (1992) Wettability. Plenum Press, New York
29. Wu W, Giese RF Jr, van Oss CJ (1955) Langmuir 11:379–382
30. Dellavolpe C, Maniglio D, Brugnara M, Siboni S, Morra M (2004) J Colloid Interface Sci 271:434–453
31. Ström G, Fredriksson M, Stenius P (1987) J Colloid Interface Sci 119:352–361
32. Gonzalez-Martin ML, Janczuk B, Labajos-Broncano L, Bruque JM (1997) Langmuir 13:5991–5994
33. Erbil Y (1997) In: Birdi KS (ed) Handbook of surface and colloid chemistry. CRC Press Boca Raton, Florida
34. Bryjak M, Pozniak G, Gancarz I, Tylus W (2004) Desalination 163:231–238
35. Chan CM, Ko TM, Hiraoka H (1996) Surf Sci Rep 24:1–54
36. Lieberman MA, Lichtenberg AJ (1994) Principles of plasma discharges and materials processing. Wiley, New York
37. Park JB, Oh JS, Gil EL, Kyoung SJ, Lim JT, Yeom GY (2010) J Electrochem Soc 157:D614–D619
38. Siow KS, Britcher L, Kumar S, Griesser HJ (2006) Plasma Proc Polym 3:392–418
39. Bhusari D, Hayden H, Tanikella R, Allen SAB, Kohl PA (2005) J Electrochem Soc 152:F162–F170
40. Inagaki N, Tasaka S, Hibi K (1992) J Polym Sci A 30:1425–1431
41. Alves P, Pinto S, Kaiser JP, Bruinink A, de Sousa HC, Gil MH (2011) Coll Surf B 82:371–377
42. Kogoma M, Turba G (1986) Plasma Chem Plasma Proc 6:349–380
43. Naddaf M, Balasubramanian C, Alegaonkar PS, Bhoraskar VN, Mandle AB, Ganeshan V, Bhoraskar SV (2004) Nucl Instr Meth Phys Res B 222:135–144
44. Kamgang JO, Naitali M, Herry JM, Bellon-Fontaine MN, Brisset JL, Briandet R (2009) Plasma Sci Technol 11:187–193
45. Gerenser LJ (1993) J Adhes Sci Technol 7:1019–1040
46. Bellel A, Sahli S, Raynaud P, Segui Y, Ziari Z, Eschaich D, Dennler G (2005) Plasma Process Polym 2:586–594
47. Faibish RS, Yoshida W, Cohen Y (2002) J Colloid Interface Sci 256:341–350
48. Ruckenstein E, Gourisankar SV (1984) J Coll Interface Sci 101:436–451
49. Kwok SCH, Wang J, Chu PK (2005) Diamond Relat Mater 14:78–85
50. Agathopoulos S, Nikolopoulos P (1995) J Biomed Mater Res 29:421–429
51. van Oss CJ (1990) J Protein Chem 9:487–491
52. van Oss CJ (2003) J Mol Recognit 16:177–190
53. Vijayanand K, Deepak K, Pattanayak DK, Rama Mohan TR, Banerjee R (2005) Trends Biomater Artif Org 18:73–83
54. Sharma CP (2001) J Biomater Appl 15:359–381
55. Brunauer S, Deming LS, Deming WE, Teller E (1940) J Am Chem Soc 62:1723–1732
56. Guggenheim EA (1966) Application of statistical mechanics. Clarendon Press, Oxford
57. Anderson RB (1946) J Am Chem Soc 68:686–691

58. De Boer JH (1968) The dynamical character of adsorption. Clarendon Press, Oxford
59. Aranovich G, Donohue M (1998) J Colloid Interface Sci 200:273–290
60. Gregg SJ, Sing KSW (1982) Adsorption, surface area and porosity. Academic Press, London
61. Donohue MD, Aranovich GL (1998) Adv Colloid Interface Sci 76–77:137–152
62. Cosutchi AI, Hulubei C, Stoica I, Dobromir M, Ioan S (2008) e-Polymers 68:1–15
63. Chae B, Lee SW, Lee B, Choi W, Kim SB, Jung YM, Jung JC, Lee KH, Ree M (2003) J Phys Chem B 107:11911
64. Klee D, Höcker H (2000) Adv Polym Sci 49:1–57
65. Ikada Y (1984) Adv Polym Sci 57:103–140